

Determination of aerodynamic coefficients and visualisation of the flow around the axisymmetrical model by experimental and numerical method

Slavica Ristić, PhD (Eng)¹⁾
Dušan Matić, BSc (Eng)¹⁾
Aleksandar Vitić, BSc (Eng)¹⁾

Test of the flow field around the axisymmetrical body – model of the torpedo without fins and control surfaces, was performed in the trisonic wind tunnel of the Military Technical Institute (MTI), for the speed of undisturbed flow which corresponds to the Mach number $M_\infty = 0.3$. Aerodynamic forces and moments were measured by six-component internal strain gage balance. Oil emulsion film with addition of oleic acid and TiO_2 powder were used for flow visualization in the boundary layer.

The goal of the experiment was to make comparison of the aerodynamic coefficients and flow pattern obtained by the experiment and by the simulations of the flow possible i.e. to provide reliable experimental data for the purpose of uncertainty analysis (verification and validation) of the numerical results. Fluent 6.1 was used for simulation of the flow. Drag coefficient values, which were obtained by simulation, show a relatively good agreement with the experimental results. Lift coefficient values, which were obtained by simulation, show some differences with regards to the experimental results due to the simplifications introduced into the experimental setup and numerical model. Numerical flow pattern results show very good agreement with the experimental results.

Key words: flow visualization, aerodynamical coefficient, flow pattern, boundary layer, torpedo.

Introduction

MODERN process of aircraft and missile design requires the use of a variety of theoretical, experimental and numerical methods. The experimental methods used are: measuring the aerodynamic forces and moments on the models in the wind tunnels, measuring the pressure distribution on the surface of the model and visualization of the flow around the model or real aircraft. The experiments are performed in wind tunnels and in free flight [1–8].

Computational Fluid Dynamics (CFD) has already demonstrated its capability to produce solutions of various, sometimes very complex flows of practical interest. Nowadays, the question is not so much whether a simulation of this flow can be made, but rather is the solution reliable enough for the use in design practice? The development of methods for the uncertainty analysis (verification and validation) of the numerical results of the flow simulation is not possible without the comparison of numerical and reliable experimental results. Good agreement of the numerical and experimental results shows good quality of the simulation [11–16].

Results for the aerodynamic coefficients and flow pattern in the boundary layer around the axisymmetrical model – model of the torpedo without fins and control surfaces, are shown in this paper. Measuring of the aerodynamic forces and moments by six-component internal strain gage balance VTI38A and visualization of

the flow with oil emulsion film were performed in the T38 wind tunnel in the MTI, for the speed of undisturbed flow which corresponds the Mach number $M_\infty = 0.3$ and angles of attack of the model in the range from $\alpha = -2^\circ$ to $+18^\circ$ [1–3].

Fluent 6.1 was used for simulations of the turbulent flow around the axisymmetrical body. Solver of the software is based on the finite volume method for discretization of the governing equations of the flow. Originally, simulations were performed for a wide range of Reynolds numbers and angles of attack on the body. Flows with seawater and air were examined. Only a part of the results, those concerning the simulations of the air flow, for conditions corresponding the flow conditions during the experiment in the wind tunnel, are shown in this paper [14].

Experimental and numerical results for aerodynamic coefficients and flow pattern for the flow around the axisymmetrical body – model torpedo without fins and control surfaces are shown in this paper. Torpedo model with fins and control surfaces was already tested in the wind tunnel T–38 and simulations with this more complex geometry are in progress [1, 2].

Description of the model and test equipemen

Measuring of the aerodynamic coefficients and visualization of the flow were performed in trisonic wind tunnel T–38 in the MTI. The T–38 is a blowdown,

¹⁾ Military Technical Institute (VTI), Ratka Resanovića, 11132 Belgrade

pressurized wind tunnel, with 1.5x1.5m square test section. Mach numbers ranging from 0.2 to 4.0 can be achieved in the test section, with Reynolds numbers up to 110 million per meter. A test section for subsonic and supersonic flows has solid walls. For transonic flow, a test section with porous walls is in use. Wall porosity varies between 1.5% and 8%, depending of the Mach number, which provides good quality of the flow in the test section. Run times of experiments in the tunnel can vary from 6 to 60 seconds, corresponding to stagnation pressure and Mach number.

The axisymmetrical model was made from aluminium alloy and steel. Scale of the model is 1:8, in relation to the object. Length of the model is 967 mm and its diameter is 66.6 mm. The model was fixed to the mechanism for changing the angle of attack of the model through specially designed 15° adapter and 15° bent sting. It was possible to achieve the desired pitch angle within the range from -4° to +25° [1].



Figure 1. The axisymmetrical model in the test section of the T-38 wind tunnel

For the purpose of measuring aerodynamic forces and moments, a precise six-component strain gage balance VTI38A was put inside the model.

The range of balance is 3000 N for the normal force, 3000 N for the side force, 700 N for the axial force, 300 Nm for the pitching moment and 50 Nm for the rolling moment. The accuracy of the balance is approximately 0.3% FS. Balance was calibrated before the measuring. It was set on the 50 mm diameter sting.

To provide maximal visibility of the flow visualization effects on the model body, preparation of the model was necessary. Through mechanical finishing of the model surface, satisfactory roughness of the entire surface of the model was achieved. The model was aluminized and parts that could not be aluminized were painted in black. Before the test started, a layer of acrylic putty had been placed in the hollows around the screws [2].

Description of the experiment

Determination of the aerodynamic coefficients

First phase of the experiment comprises preparation of the model and mounting of the model onto the support sting, checking of all the measuring systems and preparations concerning flow visualization. The chosen angles of attack of the model, ranging from -2° to +18°, were defined as static angles at which the model had been put before the test started. The model stays in that position during the measurement and after the flow in the test section stops.

The experimental data acquisition system in the T-38 consisted of 64 – channel Teledyne system controlled by Compaq PC. 16-bit A/D converter digitalizes data from all analogous channels. Approximate accuracy of the A/D conversion is 0.1 PS of channels. Sampling rate for all the channels was 200 samples per second. Digital data were received by Digital ALFA SERVER and written on disc for

further processing.

Data processing was performed after each blowdown by standard software T38-APS that is in use for measurement data processing in all MTI wind tunnels. Processing was performed in following phases:

- reading of the written raw data, normalization and conversion into the standard format,
- determination of the flow parameters,
- determination of the position of the model and
- determination of the aerodynamic coefficients.

Measuring of the stagnation pressure p_0 and stagnation temperature T_0 in the appeasement chamber and static pressure p_{st} in the test section of the wind tunnel, were necessary for determination of the values of the Mach and Reynolds numbers in the test section of the wind tunnel. Equations of the isentropic, incompressible fluid flow are used for determining the parameters of the undisturbed flow in the test section [1].

Two coordinate systems were used during data processing: wind tunnel and aerodynamic coordinate system. Wind tunnel, balance and relative coordinate systems were used only in computing intermediate results [1].

Visualization of the flow in the boundary layer

Oil emulsion films on the petroleum basis with addition of the oleic acid and titanium dioxide (TiO_2) powder were used for visualization of the flow on the entire surface of the model. Two techniques of oil film emulsion depositing were parallelly used during the experiment. One side of the model was covered with continual layer and the other side by dotted rings of the emulsion. A continual layer of small thickness of the emulsion was deposited by fine sponge. Dots of the emulsion were deposited by fine soft brush, immediately before the blowdown [2,4,7,15,16].

Pictures of the flow visualization effects were taken after each blowdown. The model was removed from the test section for the purpose of photographing it. Pictures of the flow patterns are obtained by Canon A70 digital camera.

Numerical simulation of the flow

Unigraphics 18.0 was used for modelling of axisymmetrical geometry – torpedo without fins and control surfaces, in its real measures. After modelling, the geometry of the body was exported to Gambit 2.0 software for basic geometry modelling and computational grid generation. Gambit was used to define a computational space around the body and to generate the computational grid. To achieve the size of the body, which will be used in simulations of the flow to be as the size of the model that was used in experiments in the wind tunnel, the whole geometry was scaled 1:8 [14].

Computational space was in a cylinder shape, which is optimal shape of a computational space for simulation of the flow around axisymmetric bodies. Dimensions of the computational space were obtained iteratively. Distance from the inlet boundary (one base of the cylinder) of the computational space to the body was equal to 1/2 of the body length, and from the outlet boundary (other base of the cylinder) of the computational space to the body was equal to 2 1/2 of the body length. Distance from the body to the symmetry boundary (envelope of the cylinder) of the computational space was bigger than 5 diameters of the body.

Tetrahedral hybrid unstructured computational grid with

variable density was generated inside the computational space for each angle of attack of the body separately. Appropriate hexahedral grid for the boundary layer was generated in the vicinity of the body.

Computational grid density and its distribution are chosen in a way to:

- give good representation of the body geometry,
- ensure that the values of the local Reynolds number y^+ are satisfactory and
- give good representation of the areas of the computational space outside the boundary layer in which large gradients of some flow variables are expected.

Depending on the angle of attack of the body, number of elements in the generated computational grids varies in the range from 348.000 to 386.000. Number of elements in computational grids increases as the angle of attack of the body increases.

For the chosen height of the computational elements in the first row next to the body, in the area of the boundary layer, and the flow speed which corresponds the one during the experiment in the wind tunnel, average value of the local Reynolds number y^+ was in the range from 40 to 48, depending on the angle of attack of the body. Maximal value of y^+ was in the range from 60 to 71, depending on the angle of attack of the body. Local Reynolds number average and maximal values increase as the angle of attack of the body increases.

Fluent 6.1 was used for simulation of the flow around the axisymmetrical. Solutions for Navier – Stokes equations are obtained through the use of Reynolds Average Solutions technique (RANS).

Segregated numerical scheme was used to obtain the solution of the flow. The flow was considered steady.

$k - \varepsilon$ RNG and $k - \omega$ standard models for turbulent stresses were used. Two turbulence models were used to compare the influences on the results of simulation of the same flow that each of these turbulence models has. Standard wall functions are used in the area of the boundary layer. Average values of local Reynolds number y^+ guarantee the correct application of the standard wall functions.

Pressure correction equation was discretized by the standard scheme, while momentum equations (Reynolds equations) and equations of the turbulence models were discretized by the second order upwind scheme. For pressure and velocity fields coupling, SIMPLE algorithm was selected.

Boundary conditions for simulation of the flow are chosen to be the same as the conditions in the wind tunnel during the experiment.

Converged solutions for integral quantities of interest were obtained after 250 iterations. Solution convergence criterion for all calculations was based on the scaled sum of the mass residuals. The value of $1 \cdot 10^{-4}$ was enough to obtain the convergence of drag coefficient and lift coefficient.

Analysis of the results

Numerical calculation of the aerodynamic coefficients

Aerodynamic coefficients and flow pattern are results of the simulations of the flow, which were performed in the Fluent 6.1. The traces of the flow patterns on the body

surface were generated for all the angles of attack of the body for which the flow was numerically simulated, i.e.

$\alpha = 0^\circ - 18^\circ$, with 2° step. Results of the simulations are presented in a table and the traces of the flow patterns are shown in the figures [14].

Results for two aerodynamic coefficients – drag coefficient C_x and lift coefficient C_z , which were experimentally obtained in the wind tunnel and by the simulations of the flow, are shown in Table 1. The experimental results for relative (wind tunnel) coordinate system are given in columns 3 and 4 and the experimental results for aerodynamic coordinate system are given in columns 5 and 6. Values of the numerically calculated coefficients are given in columns 7–10, for both turbulence models which were used.

Table 1. Aerodynamic coefficients for the axisymmetrical body – torpedo without fins and control surfaces

α°	α [rad]	Relative CS		Aerodynamic CS		Fluent $k - \varepsilon$ RNG		Fluent $k - \omega$ std	
		C_{x1}	C_{z1}	C_x	C_z	C_x	C_z	C_x	C_z
1	2	3	4	5	6	7	8	9	10
0	0	0.2289	0.03	0.2289	0.03	0.19739	0.00035	0.20236	0.00124 9
2	0.035	0.2103	0.018	0.21079989	0.0106534	0.20047	0.062924	0.2033	0.06741 8
4	0.07	0.2127	0.031	0.21434375	0.01609487	0.21137	0.13017	0.21413	0.13895
6	0.105	0.2171	0.086	0.22489682	0.06284769	0.2298	0.21856	0.23428	0.23705
8	0.14	0.2262	0.207	0.25279519	0.17352243	0.25208	0.30842	0.26141	0.34297
10	0.174	0.2222	0.349	0.2794005	0.305138	0.28739	0.42723	0.30605	0.48926
12	0.209	0.2152	0.494	0.31315918	0.43849557	0.33497	0.56248	0.36054	0.6445
14	0.244	0.2176	0.662	0.37121559	0.58973955	0.38863	0.70123	0.42986	0.83161
16	0.279	0.2134	0.879	0.44730719	0.78619135	0.46354	0.87451	0.52126	1.0423
18	0.314	0.2054	1.117	0.5403599	0.99894411	0.5577	1.0627	0.63018	1.2623

Diagrams in Figures 2 and 3, show aerodynamic coefficients C_x and C_z , obtained experimentally and by the simulations of the flow, as a function of the angle of attack change and are given as parallel.

In can be seen in the diagram given in Fig.2 that the values of the drag coefficient C_x , which are obtained by simulations of the flow, show a relatively good agreement with the experimental results, for both turbulence models used, in the range of the attack angles of the body from 2° to 8° . For angles of attack of the body bigger than 8° , C_x values obtained with the use of $k - \varepsilon$ RNG turbulence model are still in good agreement with the experimental values (up to 4% difference), while the difference between C_x values obtained with the use of $k - \omega$ standard turbulence model and experimental values increase as the angle of attack increases.

Diagram given in Fig.3 shows that the agreement between the lift coefficient C_z values obtained by simulations of the flow and experimental values are not as good as they were for drag coefficient C_x . The difference is almost equal for both turbulence models used in the range of small angles of attack (up to 280% for $\alpha = 6^\circ$, $k - \omega$ standard). For angles of attack bigger than $\alpha = 6^\circ$,

the difference between C_z values obtained with the use of $k - \varepsilon$ RNG turbulence model and experimental values decrease as the angle of attack increases (6.4% for $\alpha = 18^\circ$). The differences between C_z values obtained with the use of $k - \omega$ standard turbulence model and experimental values for angles of attack bigger than 6° are almost equal as for $\alpha = 6^\circ$ (a slight increase of the difference as the angle of attack increases can be observed).

The difference between experimental and numerical results can be explained in many ways. Prior to all, it should be pointed out that every numerical technique used for simulation of the flow introduces some errors in the results of the calculations. Uncertainty analysis of the numerical results should be performed before they are used in the design.

It is presumed that there are two basic reasons for bigger differences between experimental and numerical values. Firstly, there are simplifications that are introduced into the experimental setup and the geometry of the computational space that was used in the simulations of the flow. In the experimental setup, the influence of the model support sting was neglected and the results for the force coefficients include a part from the forces that are induced on the model support sting. On the other hand, during the generation of the computational space and grid that will be used for the simulation of the flow, model support sting was not modelled. The introduction of the sting geometry into the computational space would result in excessive growth of the number of elements in the computational grid, which could not be tolerated due to the characteristics of the computer that was used for the calculations.

The force coefficients obtained from the experiment include contribution of the forces induced on the model support sting, and those obtained from the simulation of the flow do not. From the results presented in Table 1 and Fig.3 it can be concluded that the influence of the lift force generated on the model support sting on the lift coefficient C_z is not negligible for a whole range of examined angles of attack of the model. Influence of the generated axial force on the drag coefficient C_x is smaller and limited to the angles of attack bigger than 8° , as it can be seen in Fig.2.

The second reason is, that the measured values of the drag and lift forces for small angles of attack of the model (α up to 4°) were too small comparing to the measuring range of the used balance and its accuracy level [1,2]. This can explain the fact that the experimental value for the drag coefficient C_x is bigger for $\alpha = 0^\circ$ than it is for $\alpha = 2^\circ$ or 4° and that the value of the lift coefficient C_z is not zero for $\alpha = 0^\circ$ and it is bigger then the C_z values for $\alpha = 2^\circ$ and 4° .

It is obvious that there are considerable differences between numerical results obtained by the use of different turbulence models. From the presented results it can be seen that the agreement between the numerical and experimental results was much better when $k - \varepsilon$ RNG turbulence model was used in the numerical calculations, which is in accordance with the former authors' experience with the simulations. Nevertheless, the convergence of relevant integral quantities was faster when the $k - \omega$ standard turbulence model was used.

For the drag coefficient C_x , bigger differences emerge

when the angle of attack of the body is bigger than 10° . Situation is similar for the lift coefficient C_z . Differences between the numerical results obtained with the use of these two turbulence models of this intensity are unexpected and need further study.

It can be concluded that the basic objective of the experiment is to provide reliable experimental data for the purpose of uncertainty analysis of the numerical results is only partially fulfilled. For the purpose of uncertainty analysis of the drag coefficient C_x values, experimental values which correspond the angles of attack of the bodies that are bigger than 4° and can be used because of the angle simplifications introduced into the experimental setup and accuracy level of the balance that has not influenced the experimental values of C_x greatly. Experimental values of the lift coefficient C_z cannot be used for the uncertainty analysis of C_z values, which are obtained numerically because of the influence, which the simplifications and accuracy level of the balance have introduced into the experimental values of C_z .

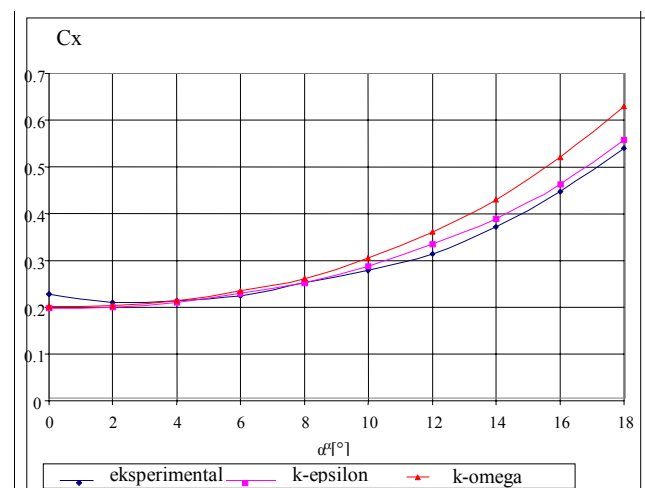


Figure 2. Diagram of the drag coefficient C_x as a function of the angle of attack

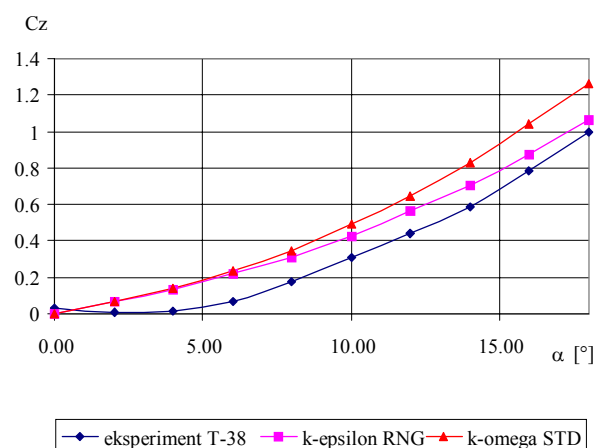


Figure 3. Diagram of the lift coefficient C_z as a function of the angle of attack

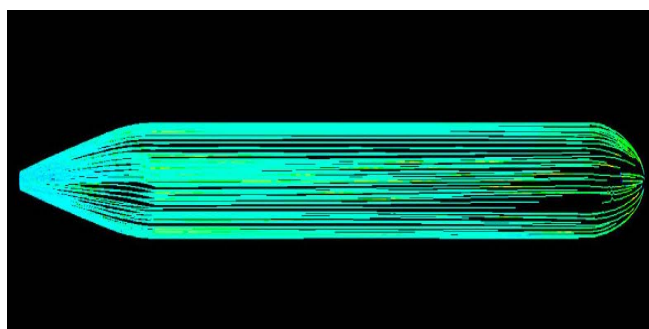
Analysis of the visualization results

Analysis of the photographs shows that the effects of the visualization after 45 seconds wind tunnel blowdown are

very good, since there was enough time to develop a good flow pattern. Low temperature in the test section of the wind tunnel caused a change of viscosity of the oil emulsion that was used for the flow visualization and so the duration of the blowdown had to be increased to the maximum for the given flow conditions.



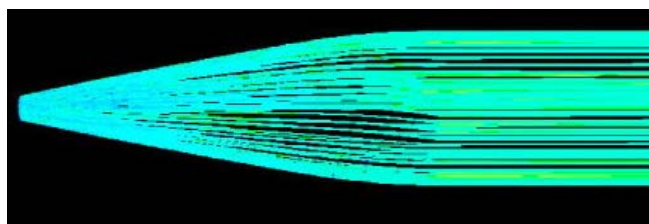
a)



b)



c)



d)

Figure 4. Flow pattern on the model obtained via experiment (a,c) and the simulation of the flow (b,d) for $M_\infty = 0.3$ and $\alpha = 0^\circ$ (side view)

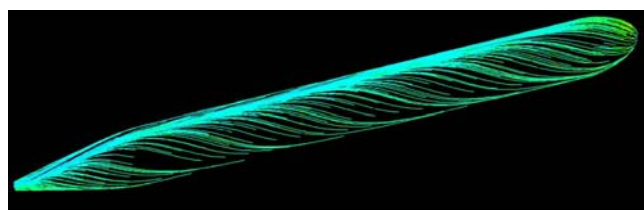
Pictures of the whole model, nose of the model and tail of the model were taken in order to compare experimental flow patterns, which correspond to different techniques of depositing the oil emulsion on the model with flow patterns and which were obtained by simulations of the flow.

Analysis of the shown photographs demonstrates an excellent agreement of the flow patterns obtained experimentally and by the simulations. Certain differences are visible in the area behind the model support sting and in its immediate vicinity because this sting is not included into the numerical model (Figures 5a, 6a and 7a). Those differences are small, which shows that the modified 15°

adapter enters smaller disturbances into the flow than the adapter, used in the previous experiments [1,2,16].



a)



b)

Figure 5. Flow pattern on the model obtained by the experiment (a) and by the simulation of the flow (b) for $M_\infty = 0.3$ and $\alpha = 8^\circ$ (side view).

Stagnation point moving as the function of the angle of attack of the model can be accurately followed in the photographs of the nose of the model (Figures 8a and 8b). Stagnation point moves from the central part of the nose towards the bottom. Photographs of the flow patterns which were taken during the experiment in the wind tunnel and figures of the flow pattern which were generated after the simulations of the flow in the Fluent, show that the comparison of the flow patterns is easier when oil emulsion is deposited in dots over the surface of the model rather than when the whole surface of the model is covered with continual layer of oil emulsion [2,3,9,15,16].

As the body during the process of the flow pattern generation in the Fluent is considered transparent, some overlapping of the flow patterns in the figures (Fig.7b) occurs, which additionally complicates the comparison with the flow pattern obtained by the experiment. In the further studies, this problem could be eliminated by the use of some post-processing software (for e.g. Field View).

Conclusion

The basic objective of the experiment, to provide reliable experimental data for the purpose of uncertainty analysis of the simulation results has been partially accomplished. For the purpose of uncertainty analysis, only the experimental values for the drag coefficient C_x can be used, for a limited range of angles of attack of the body. This is because the differences between the experimental and numerical results, beside the part which is introduced by errors that every CFD technique includes, comprises a part, which is caused by simplifications that were introduced into the experimental setup and into the numerical model, and accuracy level of the used balance. In the further studies this problem can be eliminated either by estimating the influence of the model support sting on the experimental results or by introducing the geometry of the sting into the simulations.

Visualization of the flow in the boundary layer by means of the oil emulsion films appears to be a good choice. Judging from the authors' prior experiences the experiments that include visualization of the flow with oil

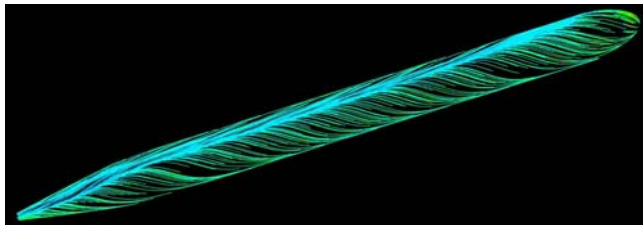
films should be performed when ambient temperature is over 20°C , if possible. Under that circumstance, the blowdown time will be much shorter, which is more economical and the flow pattern on the model surface is defined much better.

Good agreement of the flow patterns obtained by the experimental visualization of the flow in the boundary layer and by simulation of the flow confirms the possibility of the used numerical technique to produce good flow pattern.

On the bases of this experiment and references available, it can be concluded that methods of visualization are very useful for experiments that were performed in wind tunnels and for qualitative confirmation of the results that were obtained by simulations.



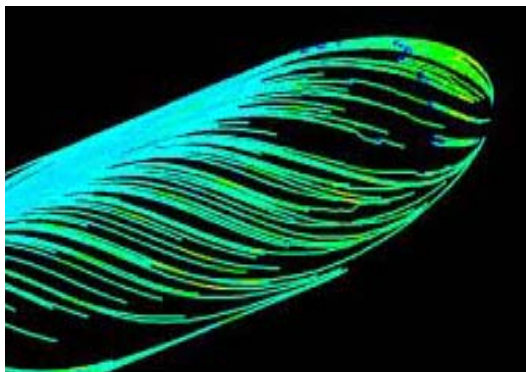
a)



b)



c)

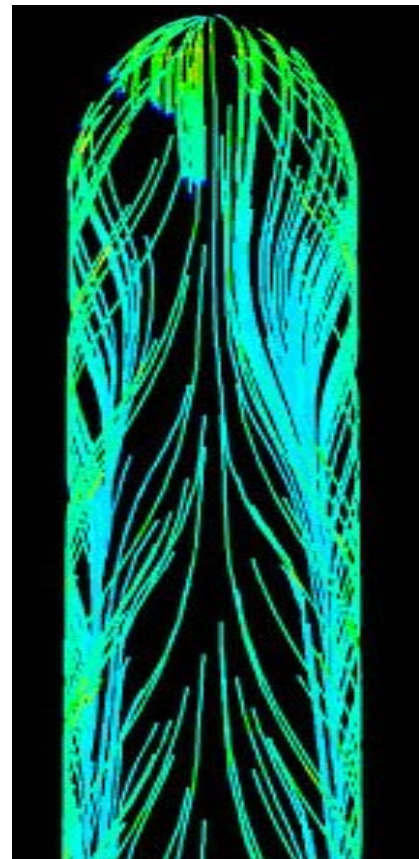


d)

Figure 6. Flow pattern on the model obtained by the experiment (a,c) and by the simulation of the flow (b,d) for $M_{\infty} = 0.3$ and $\alpha = 16^{\circ}$ (side view).

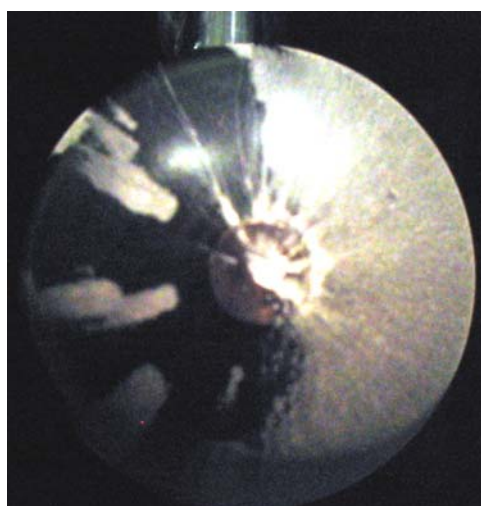


a)



b)

Figure 7. Flow pattern on the model obtained by the experiment (a) and by the simulation of the flow (b) for $M_{\infty} = 0.3$ and $\alpha = 16^{\circ}$ (top view)



a)



b)

Figure 8. Moving of the stagnation point on the nose of the model for $M_\infty = 0.3$ and $\alpha = 0^\circ$ (a) and for $\alpha = 16^\circ$ (b)

References

- [1] VITIĆ, A.: *Ispitivanje modela torpeda na Mahovim brojem $M = 0.3$ u aerotunelu T-38*, VTI - Beograd, 2003.
- [2] RISTIĆ, S.: *Vizualizacija strujanja oko modela torpeda u aerotunelu T-38 uljanim premazima*, VTI - Beograd, 2003.
- [3] RISTIĆ, S.: *Vizualizacija strujanja oko modela tela torpeda u aerotunelu T-38 uljanim premazima*, VTI - Beograd, 2004.
- [4] MARZKIRICH, W.: *Flow visualization*, Academic Press, New York, 1977.
- [5] YANG, W.J.: *Flow visualization III proc. of 3. International Symposium*, An Arbor MI, 1983, Hemisphere, New York, 1985.
- [6] SETTLES, G.S.: *Modern Developments in Flow Visualization*, AIAA Journal, 1986, Vol.24, No.8, pp.1313-1323.
- [7] RISTIĆ, S.: *Vizualizacija strujanja u aerodinamičkim tunelima*, Glasnik RV i PVO, 1990, No.1, pp.16-24.
- [8] RISTIĆ, S.: *Pregled metoda za vizualizaciju strujanja u aerodinamičkim tunelima*, KumNTI, VTI Beograd, 1999, No.3.
- [9] WILLEM, C. de LEEUW, HANS-GEORG PAGENDARM, FRITS, H.POST, BIRGIT WALTER: *Visual Simulation of Experimental Oil-Flow Visualization by Spot Noise Images from Numerical Flow Simulation*, 2001.
- [10] VAN WIJK, J.: *Spot noise Texture synthesis for data visualization*, Computer graphics, 1991, 25(4), pp.309-318.
- [11] ROE, P.L.: *Numerical Methods in Aeronautical Fluid Dynamics*, London, Academic Press, 1982.
- [12] VERSTEEG, N.K., MALALASEKERA, W.: *An Introduction to computational fluid dynamics - The finite volume method*, Longman, 1996.
- [13] FERZIGER, J.N., PERIĆ, M.: *Computational Methods for Fluid Dynamics*, Springer, Berlin, 1997.
- [14] MATIĆ, D.: *Simulacija strujanja oko obrtnog tela – modela torpeda bez stabilizatora*, VTI - Beograd, in preparation.
- [15] RISTIĆ, S., MATIĆ, D., VITIĆ, A.: *Vizualizacija i numerička simulacija strujanja oko prednjeg dela modela torpeda*, HIPNEF Vrnjačka banja, 19-21 maj 2004, Zbornik radova, str.267-273
- [16] RISTIĆ, S., VITIĆ, A., ANASTASIJEVIĆ, Z., VUKOVIĆ, Đ.: *Investigation of Support Interaction Upon Aerodynamic Characteristics of a Torpedo Model in the T-38 Wind Tunnel*, Scientific technical review, 2004, Vol. LIV, No.1, pp.50-57.

Received: 10.03.2005.

Određivanje aerodinamičkih koeficijenata i vizualizacija strujne slike oko osnosimetričnog modela eksperimentalnim i numeričkim metodama

Ispitivanje strujnog polja oko osnosimetričnog tela koje predstavlja model torpeda bez stabilizatora i kontrolnih površina je izvršeno u trisoničnom aerotunelu, u laboratorijama VTI-a, za brzinu neporemećene struje sa Mahovim brojem $M_\infty = 0.3$. Merenje aerodinamičkih sila i momenata je vršeno unutrašnjom aerovagom. Vizualizacija strujanja u graničnom sloju je realizovana premazima na bazi parafinskog ulja s dodatkom oleinske kiseline i praha TiO_2 .

Cilj eksperimenta je bio da se omogući poređenje aerodinamičkih koeficijenata i strujne slike dobijenih eksperimentom i numeričkim simulacijama strujanja, to jest da se obezbede pouzdani eksperimentalni podaci za potrebe analize tačnosti rezultata proračuna (verifikacija i validacija). Numeričke simulacije strujanja su izvedene u programu Fluent 6.1. Vrednosti koeficijenta otpora dobijene simulacijama se relativno dobro slažu sa eksperimentalnim rezultatima. Vrednosti koeficijenta uzgona dobijene numeričkim simulacijama pokazuju određena odstupanja od eksperimentalnih rezultata zbog pojednostavljenja koja su uvedena u postavku eksperimenta i numerički model. Strujna slika dobijena numeričkim simulacijama pokazuje veoma dobro slaganje sa eksperimentalnom strujnom slikom.

Cljučne reči: vizualizacija strujanja, aerodinamički koeficijenti, slika strujanja, granični sloj, torpedo.

Определение аэродинамических коэффициентов и визуализация потока около осевосимметрической модели экспериментальными и численными методами

Исследование поля потока около осевосимметрического тела, которое представляет модель торпеды, без стабилизатора и контрольных площадей, проведено в трёхзвуковой трубе в лабораториях ВТИ, для скорости ненарушенного потока со числом Маха $M_\infty = 0.3$. Измерение аэродинамических сил и моментов проведено при помощи внутренних аэровесов. Визуализация потока в пограничном слое реализована масляными плёнками на основе парафинового масла с прибавлением олеиновой кислоты и порошка TiO_2 . Цель этого эксперимента была воспрепятствовать сравнению аэродинамических коэффициентов и картины потока, полученных путём эксперимента и численных моделирований потока, то есть обеспечить достоверные экспериментальные данные нужные для анализа точности результатов расчёта (проверка подлинности и полномочий). Численные моделирования потока проведены в программе Флуент 6.1. Величины коэффициента сопротивления получены путём моделирования относительно хорошо согласовываются с экспериментальными результатами. Величины коэффициента подъёмной силы получены путём численных моделирований указывают на определённые отклонения от экспериментальных результатов из-за упрощений, которые введены в предположение эксперимента и в численную модель. Картина потока, получена путём численных моделирований, указывает на очень хорошее согласование с экспериментальной картиной потока.

Ключевые слова: визуализация потока, аэродинамические коэффициенты, картина потока, пограничный слой, торпеда.

Détermination des coefficients aérodynamiques et visualisation de l'image du courant autour du modèle axisymétrique à l'aide des méthodes expérimentales et numériques

La recherche du champ de circulation autour d'un corps axisymétrique qui représente le modèle de torpille sans stabilisateur et les surfaces de contrôle était effectuée dans la soufflerie aérodynamique trisonique des laboratoires de VTI, pour la vitesse du courant non perturbé ayant le numéro de Mach $M_\infty = 0.3$. Les forces aérodynamiques et les moments ont été mesurés à l'aide de la balance aérienne intérieure. La visualisation du courant dans la couche limite était réalisée au moyen des enduits à la base de l'huile de paraffine avec l'additif de l'acide d'oléine et de la poudre TiO_2 . Le but d'essai était de permettre la comparaison entre les coefficients aérodynamiques et l'image du courant obtenus pendant cet essai et par les simulations numériques du courant, c'est-à-dire d'assurer les données sûres d'essai pour les besoins d'analyse d'exactitude du calcul (vérification et validation). Les simulations numériques du courant ont été réalisées à partir du programme Fluent 6.1. Les valeurs du coefficient de résistance, obtenus par les simulations, sont en assez bon accord avec les résultats d'essais. Les valeurs du coefficient de poussée, obtenues par les simulations numériques, démontrent certaines différences par rapport aux résultats d'essais dus aux simplifications introduites dans l'installation expérimentale et le modèle numérique. L'image du courant, obtenue par les simulations numériques, démontre très bon accord avec l'image expérimentale de courant.

Mots clés: visualisation du courant, coefficient aérodynamique, image de courant, couche limite, torpille.